

Holographic data storage using photopolymer

Ken Y. Hsu, Shiuan-Huei Lin, Wha Tzong Whang¹, and Wei Zheng Chen¹

Institute of Electro-Optical Engineering

¹Institute of Materials Science and Engineering

National Chiao Tung University

Hsin-Chu, Taiwan, R.O.C.

ABSTRACT

We present our studies on a photopolymer of poly(methyl methacrylate) (PMMA) doped with phenanthrenequinone (PQ) molecules. We describe their characteristics for holographic data storage, including photo-sensitivity, material M/#, angular selectivity, dynamic exposure schedule, absorption and scattering effect. Experimental demonstrations on multiple digital data pages stored in a polymer cube are presented.

Keywords: Photopolymer material, PQ:PMMA, Holographic data storage, M/#, Angular selectivity

1. INTRODUCTION

Holographic data storage has been considered as one of the next generation information storage technologies because of its distinct advantages of large storage capacity and fast data access rate. By using a suitable multiplexing scheme, thousands of pages of optical information can be superimposed and recorded onto one location of a recording medium. And the recorded information can be readout in a page format with ultra-high data rate. Holographic data storage systems with high storage capacity, high data readout rate, high image quality, and low bit error rate have been proposed and demonstrated [1-6]. The main components for holographic data storage systems are optical spatial light modulators (SLM) and holographic recording media. The SLMs are used as the interface devices for optical data input and output. Because of the rapid advances in liquid crystal display (LCD), digital mirror devices (DMD), and charge-coupled devices (CCD), input and output data page with one million bits per frame is achievable. The key issue for the success of holographic memory then becomes whether there are good recording medium. The crucial characteristics for a good holographic material include high sensitivity for optical exposure, large dynamic recording range, easy to fabricate of large area or volume with high optical quality (or, low scattering noise). So far, the most popular materials for volume holographic storage are photorefractive crystals and photopolymers [7-10]. Iron-doped lithium niobate crystals have been used in most demonstration systems [11-13]. Large volumes ($1 \times 1 \times 4 \text{ cm}^3$) or areas (disks with 2 inch diameter and 1 cm thickness) Fe:LiNbO₃ crystals with high optical quality are commercially available. These crystals have large dynamic range of refractive index so that more than ten thousands of optical page information can be recorded in a single location of the crystal. Also, thermal or optical techniques can be applied to this material for the fixing of holograms to achieve a non-volatile storage. However, the main disadvantage of using this material are that crystal growth requires dedicated crystal growing machine. And it takes long time (typically it is longer than one week for one run) for material preparation. It is inconvenient when one wants to change impurities and doping concentration to investigate its effects on the recording and fixing characteristics. On the other hand, photopolymers with different material components are relatively easy to fabricate. Photopolymer with different material components can be synthesized easily. Furthermore, it is easily to fabricate the materials into either a disk or cube form for different system requirements. These versatile characteristics of photopolymer make it an attractive material for holographic data storage studies [14-18]. In this paper we present our investigations on the bulk blocks of phenanthrenequinone- (PQ-) doped poly(methyl methacrylate) (PMMA). The blocks consist of PMMA, the host matrix doped with PQ molecules as the photosensitive element. In next sections, we will first describe the material preparation for the thickness from 1.2 mm to 10 mm. Then, we will present their characteristics for holographic data storage including, optical transmission quality, exposure sensitivity, the M/# number [19], and the Bragg angle selectivity. Multiple storage of 250 holograms in a single spot will be experimentally demonstrated.

2. MATERIAL PREPARATION

Our PMMA host matrix were made from the thermally chain reaction of polymerization of MMA monomers by using thermal initiator azobisisobutyronitrile (AIBN). The polymer blocks were made by two stages at different temperatures. In the first stage, samples were prepared by dissolving the initiator, AIBN (~0.5%) and PQ molecules (up to 0.7%) in solvent MMA. The solution was purified to remove the un-dissolved particles and thus reducing light scattering centers. The purified solution was poured into a square glass tube and then put in a pressure chamber at room temperature for about 120 hours until the solution turned into homogeneously viscid. During this stage, because of the slow polymerization at low temperature, nitrogen molecules released from the thermo-decomposition of AIBN and heat produced from the chain propagation of the MMA monomers could leave the glass tube completely. Therefore, there were no residual air bubbles left in the sample. In the second stage, the temperature of the chamber was elevated to 45 °C for 24 hours to accelerate the thermo-decomposition rate of AIBN. Chain reaction was accelerated and the polymerization was completed. Then the sample became a solid block and high-optical-quality polymer cubes are therefore obtained. The final shape of the blocks were determined by the geometry of the glass tube, which can be in the range from 1 x 1 to 2.5 x 2.5 cm² with thickness of 1-25 mm. In following sections, all polymer samples used are doped with 0.6% PQ molecules.

3. OPTICAL QUALITY OF THE SAMPLES

Figure 1 shows a photograph of our PQ:PMMA samples. It appears to be clear, with good optical quality and uniform transmission. Figure 2 shows the photograph of a directly transmitted image through a 4.8-mm thick block. The image retains the same quality as the illuminating image. For the application of volume holographic storage, thousands of pages are superimposed on a single location of a thick recording material. As the number of recording pages becomes large, the diffraction efficiency of each hologram is very weak (typically less than 10⁻⁶) and particular attentions must be taken to keep material scattering noise to be minimum. Thus it is very important to grow a material with high homogeneity in the refractive index. In this aspect, our technique of pre-polymerization before the photochemical reaction seems to produce satisfactory samples.

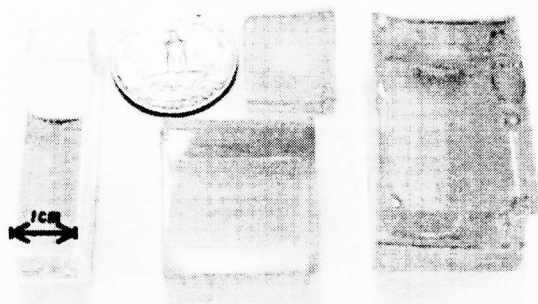


Figure 1. A photograph of our PQ:PMMA samples

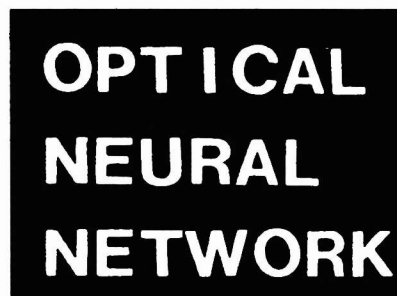


Figure 2. Photograph of a directly transmitted image through a 4.8-mm thick block

Our PQ:PMMA blocks appear to be yellow color. We have measured the optical transmission of the different thick samples in the visible range. The samples possess strong absorption below blue wavelength (<450 nm). They are totally transparent for red and near infrared wavelengths (>540 nm). In the following experiments we used an argon laser with the wavelength 514.5 nm. At this wavelength the absorption coefficient is about 2.7 cm⁻¹.

In order to explore the capability of our PQ:PMMA samples for high density holographic memory we have measured the dynamic range of the refractive index of a 4.8-mm thick sample. Two beams of collimated light derived from an argon laser were symmetrically incident into the sample with an intersection angle of 32 degrees outside the sample. The grating diffraction efficiency is measured in real-time by use of a weak 632.8-nm He-Ne-laser beam at Bragg-matched angle. The resulting curve is shown in figure 3. It is seen that the diffraction efficiency reaches the maximum of 60% for the exposure energy of 0.3 J/cm² and then it begins to drop for further exposure. At this situation we saw a distorted pattern of the

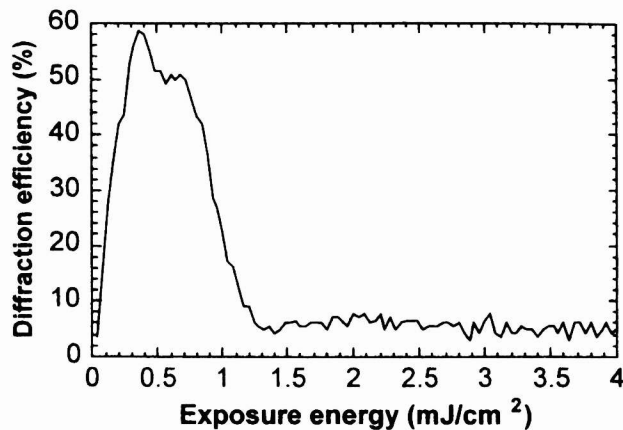


Figure 3. Recording dynamics of a single grating in 4.8- mm thick polymer sample.

transmitted beams. We believe that this drop effect of the diffraction efficiency is caused by the fanning gratings, which are induced during the recording procedure. In the thick samples, the scattering beams induced by the scattering centers or the non-uniform refractive index have long interaction length. As a result, the noise gratings are accumulated and become strong. Thus, most energy of the incident light are scattered into fanning beams and the directly transmitted beams are distorted very seriously. Figure 4 shows the photography of the directly transmitted image of Fig.2 after illuminated the sample for 100sec. Comparing these two figures it can be seen that fanning effect causes a serious distortion to the transmitted image. The implication of the fanning effect on holographic data storage is that the exposure time for each recording cannot be too long, otherwise image distortion occurs.



Figure 4. Photograph of the directly transmitted image of Fig.2 after illumination for 100sec.

We have performed an experiment to investigate the fanning effect. A collimated laser beam with 4 mW/cm^2 and 6-mm diameter was incident on the PQ:PMMA block. We measured the transmitted power as a function of time. As more exposure continued the directly transmitted power became less and less. If we defined the fanning efficiency as the total power scattered outside the beam diameter divided by the initially transmitted beam power, then the dynamics of the fanning is shown in Figure 5. It can be seen that the fanning efficiency is almost close to 70% after the exposure energy of 2.08 J/cm^2 . This implies that, in order to avoid the buildup of the beam fanning, the total exposure of a single recording should be less than 2.08 J/cm^2 . This sets up an upper limit for the exposure time.

4. THE M/# OF PQ:PMMA SAMPLES

The M/# has been used as a metric for characterizing the storage capability of a holographic storage system. The M/# is defined by the relation $\eta_{final} = (M\#/N)^2$, where N is the total number of holograms recorded in one spot of the medium

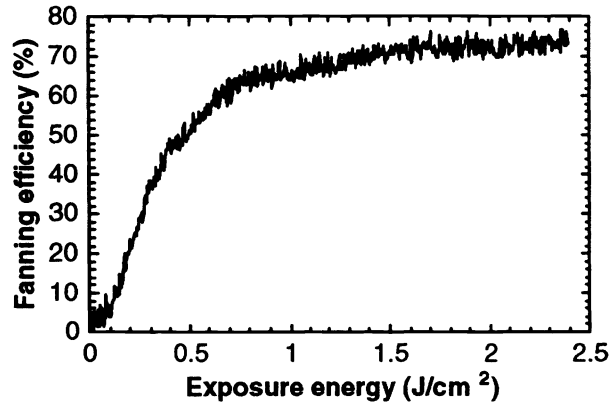


Figure 5. Dynamics of the fanning grating formation for 4.8-mm thick sample.

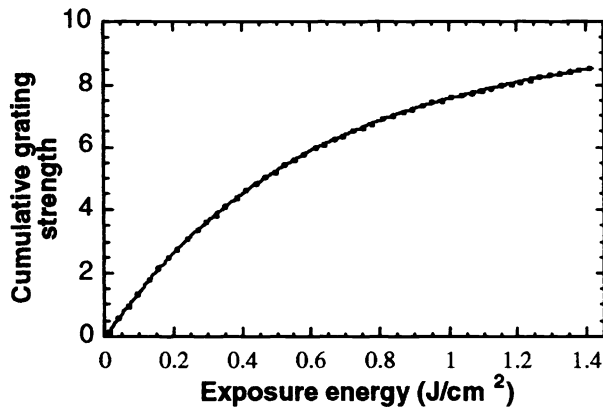


Figure 6. Cumulative grating strength as a function of exposure energy for varying thicknesses.

and η_{final} is the diffraction efficiency of each hologram (assuming equal diffraction efficiency for each hologram). The allowable minimum diffraction efficiency is determined by the light detection capability of CCD devices. Thus, for a selected CCD, larger $M/\#$ of the recording medium implies larger storage capacity of the system.

Once the polymer sample has been made, the dynamic range of the material is a common criterion to characterize the material ability for multiple storage in a single recording area. To see the role of thickness variations on the dynamic range, we have performed experiments with peristrophically multiplexed hologram storage by rotating the sample block [20]. Three hundred and fifty-five plane wave holograms were recorded with equal exposure energy ($\sim 8\text{mJ}/\text{cm}^2$) at a single location of the polymer samples. For each sample, the diffraction efficiency of each hologram was measured, and the square roots of the measured diffraction efficiencies were summed up to plot a running curve of the cumulative grating strength (defined as $C = \sum_{i=1}^N \sqrt{\eta_i}$, N is the total number of exposed holograms) with respect to the exposure order. The resulting curve for a 4.8-mm-thick polymer block is given in Figure 6. The final value of the cumulative grating strength is related to the $M/\#$ of the polymer.

The curve in Figure 6 is used to estimate the dynamic range of this polymer material. In order to model the temporal behavior of the recording, we have performed curve fitting for the running curve. The curve was represented by an exponentially growing formula (solid lines in Figure 6), and is given by the following form:

$$C = C_{\text{sat}} (1 - \exp(-E/E_{\tau})) \quad (1)$$

where C_{sat} represents the saturation value of the grating strength and E_{τ} is the characteristic response exposure energy constant. According to the definition of the $M/\#$ ($\eta_{\text{final}} = (M/\#)^2$) for the photorefractive material, the saturation value of the cumulative grating strength is related to the $M/\#$ of the polymer one. Thus, we also call the saturation value of the cumulative grating strength as the $M/\#$ for photo-polymer. The $M/\#$ is a system metric for a holographic memory systems. It depends on the experimental conditions such as material thickness, recording geometry, and physical parameters. For example, the $M/\#$ of our photopolymer with respect to the sample thickness is shown in Figure 7. As shown in the figure, the $M/\#$ increases linearly with the thickness of the polymer sample. We have also calculated the dependence of the exposure energy constant with respect to the sample thickness. The response energy constant increases as the thickness increases. This phenomenon may result from the material absorption. Because of the absorption, light beams are depleted as they propagated through the sample such that the interference fringes become weaker and weaker near the end of the sample.

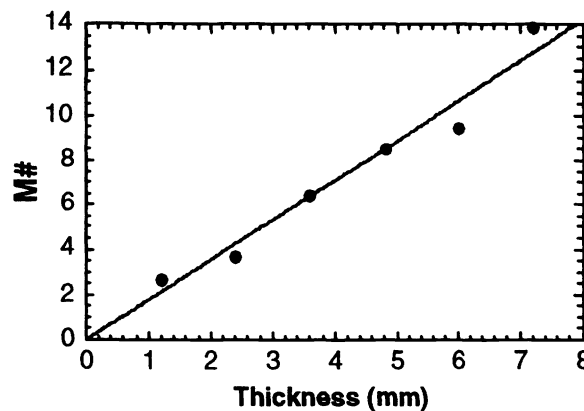


Figure 7. Dynamic range as a function of sample thickness.

5. ANGULAR SELECTIVITY

Volume holographic memories by the angle-multiplexing technique require a small width of Bragg angular selectivity $\Delta\theta$, which is the angular displacement from the peak position such that the diffraction efficiency is reduced to first null. (Here, we took 1% of its maximum value as the null in our experiments.) High angular selectivity allows large storage capacity in a angle-multiplexed holographic data storage. For a uniform refractive index change, the angular width $\Delta\theta$ can be approximately expressed as

$$\Delta\theta = \frac{\sqrt{n^2 - \sin^2 \theta_R}}{\cos \theta_R} \frac{\lambda \cos \theta_S}{d \sin(\theta_R + \theta_S)} \quad (2)$$

where λ is the wavelength (514.5-nm Argon laser), d is the thickness of the sample, n is the refractive index, and θ_S and θ_R are the incident angles of the signal and reference beams, respectively. To examine the dependence of the angular width with respect to the sample thickness, we have performed experiments to monitor the diffraction efficiency of a weak hologram with respect to the angular displacements. The rotation of the reading beam is achieved by using a telescope optical setup and a rotating mirror. The angular selectivity curves for different sample thicknesses are shown in Figure 8. It can be seen that the diffraction for the 1.2- mm-thick sample has a clear profile of the sinc-squared distribution. However, holograms of thicker samples have distorted Bragg selectivity curves, in which the nulls of the sinc-squared function can not be detected clearly. We believe that this phenomenon may result from the non-uniform refractive index change, which is generated by the absorption inside the polymer. We plot the angular bandwidth as a function of the sample thickness, which is shown in

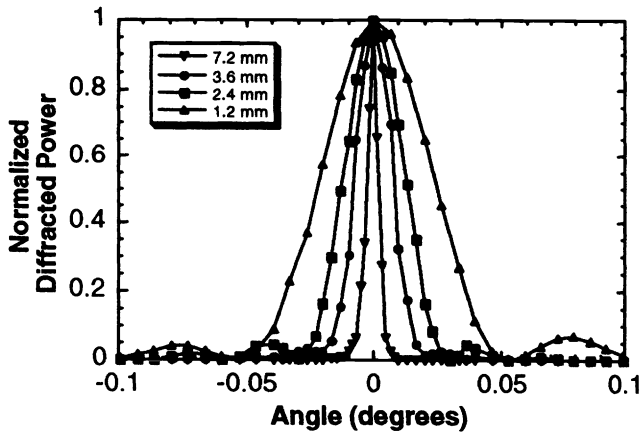


Figure 8. Bragg selectivity curves for varying thicknesses.

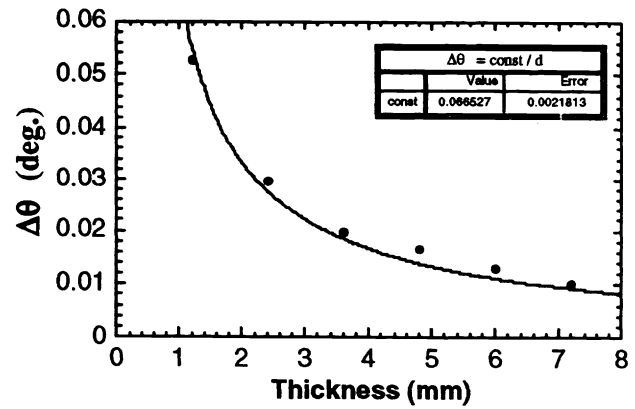


Figure 9. Angular bandwidth as a function of thickness

Figure 9. By fitting the curve with the relation (2) and the geometric parameters of $\theta_s = \theta_R = 16$ degrees, the refractive index of the polymer can be estimated as 1.23. This value is in coincide with our observation for the Fresnel reflection of the polymer cube (~20%).

6. EXPOSURE SCHEDULE FOR MULTIPLE STORAGE

We have also measured diffraction efficiency of each hologram from 355 peristrophically (1-degree rotation between holograms) multiplexed holograms for a 4.8-mm thick sample. These holograms were recorded with equal exposure energy. In the beginning, holograms possess equal diffraction efficiencies and then it decreases with the exposure order. It represents that the material exhibits a quasi-linear exposure response until the material saturates. To alleviate these non-uniformity in diffraction efficiency, a special recording schedule to compensate for the effect of the material saturation should be used.

For a given sample, allocating the dynamic range of the polymer material equally can equalize the grating strength for each hologram. The corresponding exposure energy for each equal hologram can be assigned by mapping the grating strength for each hologram into the corresponding point on the horizontal axis in Figure 6 using the relation of the transfer curve. Analytically, by differentiating Eq.(1), the growth rate of the cumulative grating as a function of the exposure energy can be obtained. Therefore, assuming that each exposure energy is very small (compare with the dynamic range), the desired exposure schedule can be written as

$$t_n = R \frac{E_\tau}{I} \exp\left(\frac{1}{E_\tau} \sum_{i=1}^{n-1} E_i\right) \quad (3)$$

where t_n is the exposure time of the n-th hologram, R is the ratio of the desired grating strength with respect to the saturation grating strength, E_τ is the response exposure energy constant from Eq. (1), E_i is the exposure energy for recording the i-th hologram, and I is the intensity of the incident light.

For a 4.8-mm thick sample, an exposure schedule for 350 holograms was calculated by Eq.(2) with the incident intensity of 2-mW/cm². It can be obtained that the exposure time for each hologram grows up as the sample exposure order is increased. The diffraction efficiencies of the 350 holograms that were recorded with this special schedule are shown in Figure 10. It can be seen that the diffraction efficiencies possess a pretty uniform distribution.

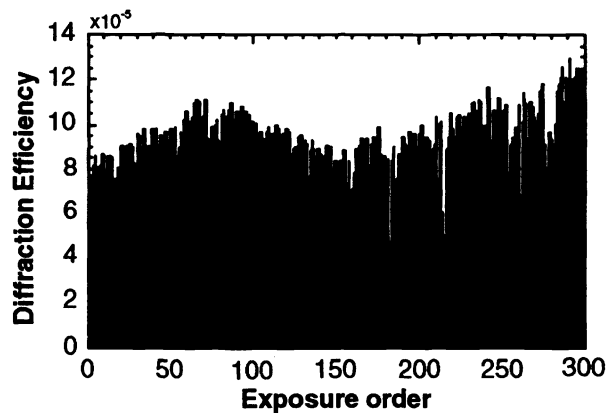


Figure 10. Diffraction efficiency as a function of exposure order with scheduled exposure.

7. MULTIPLE HOLOGRAMS STORAGE EXPERIMENTAL DEMONSTRATION

Subsequent exposures cause an erasure of the previously recorded holograms in photorefractive materials; however, in many photo-polymer materials, repeated exposure causes saturation. We have performed a multiple-holograms storage experiment on our polymer tube. A $1 \times 1 \times 5$ -cm³ polymer cube with 0.6% PQ were used in our experiment. The schematic diagram of the optical setup is shown in Figure 11. The reference and signal beams were incident into the cube at the adjoin sides of the cube. The intensity for each beam was 2 mW/cm^2 . Angle multiplexing was achieved by using a telescope structure and rotating mirror M1, which was introduced in the arm of the reference beam. Two hundred and fifty Fresnel holograms of a chessboard pattern, which was shown on a Liquid Crystal Television (LCTV) with resolution of 320×240 pixels, were recorded in a single location. There was a 2-s delay before each exposure to allow the rotation stage to settle completely. Each step of the angle separation was about 0.02° , which was the limitation of our rotation stage.

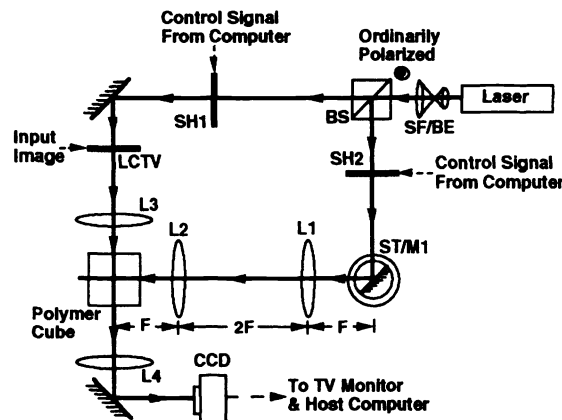


Figure 11. Schematic diagram of the optical setup to store 250 Fresnel holograms using angle-multiplexing.

The exposure time of each hologram was conducted by the recording schedule discussed in above section with the response exposure energy constant of 1.6 Jules/cm^2 . The original and 11 reconstruct images are shown in Figure 12. It is seen that the reconstructed images have good fidelity as the original image. Because the whole image can be reconstructed for such a 1-cm thick block, it implies that shrinkage is not a serious problem in our sample as that in other photo-polymerization materials. To explain this phenomenon, we briefly discuss the physical mechanism involved in our samples. Under light

illumination, PQ molecules became radicals and bonded with a single monomer, MMA. Chemical analysis showed that the residual monomer MMA in our samples is about 10%. When light distribution is not uniform, the primary chemical bond reaction occurs in the bright region. Free PQ and MMA molecules then diffuse from the dark into the bright regions due to a spatial variation of the density level. Consequently, the difference between the refractive index of the polymer matrix in dark region and that of PQ-MMA compounds in bright one is created, i.e. a phase grating. The matrix of host polymer was not influenced by light distribution and the minimal shrinkage effect was therefore achieved. Performing experiment with light-illumination on yellow mixture liquid of MMA monomers and PQ molecules confirmed this process. We observed that the compound was still liquid, but colorless; while we also observed in solid sample. This implies that PQ molecules did not cause photo-induced polymerization, instead they bonded with residual MMA monomers. In a previous paper [18], it was shown that thermal treatment could increase the diffraction efficiency of the PMMA polymer material. We believe that this effect may result from thermal-degradation of residual MMA monomers. The average diffraction efficiency of our holograms was measured as $\sim 3 \times 10^{-6}$. It is coincide to our predictions from the $M/\#$.

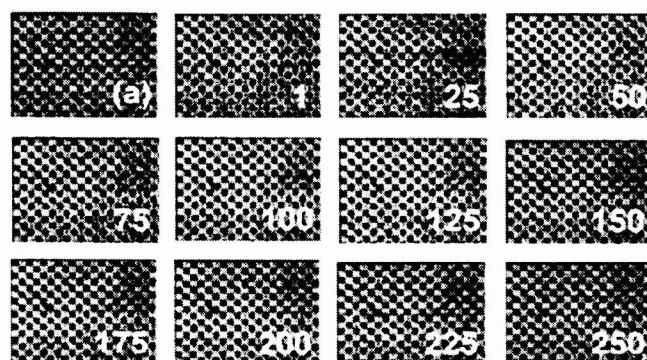


Figure 12. Photographs of an original (a) and eleven images reconstructed from 250 holograms.

Another important effect that should be concerned during the multiple recordings is the fanning noise. To examine the fanning effect during multiple recordings, Figure 6 was transferred to the dynamics of the cumulative fanning grating strength. With a curve fitting procedure, the dynamics of the noise grating can be written as

$$C_{noise} = C_{nsat} (1 - \exp(-E/E_{nr})) \tag{4}$$

where C_{nsat} represents the saturation value of the noise grating strength and E_{nr} is the characteristic response exposure energy constant for the noise grating. Comparing the growth rates for image and noise gratings by taking derivatives of the relations (1) and (4), the ratio of the signal grating strength with respect to the fanning noise one at the beginning of the grating formation can be expressed as

$$S/N = \frac{C_{sat} E_{nr}}{C_{nsat} E_{\tau}} \exp \left[-E \left(\frac{1}{E_{\tau}} - \frac{1}{E_{nr}} \right) \right] \tag{5}$$

where S/N is the ratio of the signal grating amplitude with respect to the fanning noise grating amplitude. From relation (5) it can be seen that the signal-to-noise ratio increases as the exposure energy increases. Therefore, this relationship puts an upper limit on the exposure energy for each hologram. Furthermore, the maximum number of stored holograms can be found if the required S/N ratio is given.

8. CONCLUSION

We have presented a method for synthesizing high-optical-quality photopolymer cube for volume holographic data storage. The characteristics including, the fanning effect, angular sensitivity, and $M/\#$, of the volume holographic recording with different thickness have been investigated. The $M/\#$ as large as ~ 14 and angular sensitivity $\Delta\theta$ as small as ~ 0.01

(outside sample) have been observed in 7.2-mm thick sample. These characteristics provide large dynamic range for large number storage of volume hologram. We have experimentally demonstrated a volume storage of 250 holograms in a 1x1x5-cm³ cube sample.

ACKNOWLEDGEMENT

We gratefully acknowledge the support of the National Science Council, Taiwan, R.O.C. under contract NSC 88-2215-E-009-008 for this research.

REFERENCES:

- [1]. F. H. Mok, "Angle-multiplexed storage of 5000 holograms in lithium niobate", *Opt. Letts.*, Vol. 18, pp.915-917, 1993.
- [2]. P. Gunter, J. P. Huignard Ed., "Photorefractive materials and their applications I", Springer Verlag 61, Berlin 1988.
- [3]. B. L. Booth, "Photopolymer material for holography", *Appl. Opt.*, Vol. 14, pp.593-601, 1975.
- [4]. C. P. Yang, S. H. Lin, M. L. Hsieh, K. Y. Hsu, and T. C. Hsieh, "A holographic memory for digital data storage," *Int'l J. of High Speed Electronics & Systems*, Vol. 8, No. 4, 749-765, 1997.
- [5]. P. Yeh, A. E. Chiou, P. Beckwith, T. Chang and M. Khoshnevisan, "Photorefractive Nonlinear optics and optical computing", *Opt. Eng.*, Vol. 28, pp.328-343, 1989.
- [6]. D. Psaltis, D. Brady and K. Wagner, "Adaptative optical networks using photorefractive crystals", *Applied Optics*, Vol. 27, pp.1752-1759, 1988.
- [7]. F. P. Laming, "Holographic grating formation in photopolymers-polymethylmethacrylate", *Polymer Engineering and Science*, Vol. 11, pp.421-425, 1971.
- [8]. S. Piazzolla and B. K. Jenkins, "Holographic grating formation in photopolymers", *Optics Letters*, Vol. 21, pp.1075-1077, 1996.
- [9]. L. Hesselink, S. Redfield, " Photorefractive holographic recording in stornium barium niobate fibers", *Opt. Lett.*, Vol. 13, pp.877-879, 1988.
- [10]. D. L. Staebler, W. . Burke, W. Phillips, J. J. Amodei, "Multiple storage and erasure of fixed holograms in Fe-doped LiNbO₃", *Appl. Phys. Lett.*, Vol. 26, pp.182-184, 1975.
- [11]. D. Psaltis, "Parallel optical memories", *BYTE Sept.*, pp.179-182, 1992.
- [12]. F. T. S. Yu, S. Wu, A. W. Mayers and S Rajan, "Wavelength multiplexed reflection matched spatial filters using LiNbO₃", *Opt. Commu.*, Vol. 81, pp.343-350, 1991.
- [13]. G. A. Radkujic, V. Leyva and A Yariv, "Optical data storage by using orthogonal wavelength-multiplexed volume holograms", *Opt. Lett.*, Vol. 17, pp.1471, 1992.
- [14]. J. M. Cariou, J. Dugas, L. Martin, and P. Michel, "Refractive-index variations with temperature of PMMA and polycarbonate", *Applied Optics*, Vol. 25, pp.334-336, 1986.
- [15]. A. Bloom, R. A. Bartolini, and P. L. K. Hung, "The effect of polymer host on volume phase holographic recording properties", *Polymer Engineering and Science*, Vol. 17, pp.356-358, 1977.
- [16]. H. Franke, "Optical recording of refractive-index patterns in doped poly-(methyl methacrylate) films", *Applied Optics*, Vol. 23, pp. 2729-2733, 1984.
- [17]. A. Pu, K. Curtis and D. Psaltis, "Exposure schedule for multiplexing holograms in photopolymer films", *Opt. Eng.*, Vol. 35, pp.2824-2829, 1996.
- [18]. G. J. Steckman, I. Solomatine, G. Zhou, and D. Psaltis, "Characterization of phenanthrenequinone-doped poly(methyl methacrylate) for holographic memory", *Optics Letters*, Vol. 23, pp.1310-1312, 1998.
- [19]. F. Mok, G. Burr, and D. Psaltis, "A system metric for holographic memory systems", *Opt. Lett.*, Vol. 21, pp.886-888, 1996.
- [20]. K. Curtis, A. Pu and D. Psaltis, "A method for holographic storage using peristrophic multiplexing", *Opt. Lett.*, Vol. 19, pp.993-995, 1994.